Int. J. Multiphase Flow Vol. 15, No. 2, pp. 269–278, 1989
Printed in Great Britain.

0301-9322/89 $3.00 + 0.00

REACTING SOLID PARTICLES IN ONE-DIMENSIONAL NOZZLE FLOW

S. S. GOKHALE and T. K. BOSE
Department of Aerospace Engineering, Indian Institute of Technology, Madras, India

(*Received* 26 *September* 1986; *in revised form* 15 *October* 1988)

Abstract—A fully conservative explicit scheme for a solid-particle-laden gas flow in a convergent–divergent nozzle is studied numerically as a direct time-dependent problem for a one-dimensional flow. The initial conditions at $t = 0$ are taken from the similarity solution. The boundary conditions at the nozzle inlet are determined by taking an arbitrary large cross-section at the first grid point before the nozzle inlet and are held constant with time. The exit boundary conditions are obtained at the grid point next to the exit plane from the values extrapolated at the exit plane. The particle burning rate is assumed to be a function of pressure. A time-dependent predictor–corrector formulation with a fourth-order damping term is used. Convergence of the result is assumed when the throat Mach number change is <0.0001, generally in $\leqslant 400$ time steps.

Key Words: reacting particles, solid particles, nozzle flow

1. INTRODUCTION

Large particles entrained in a rocket exhaust contribute to momentum degradation and component erosion (Hess 1985). The problem is particularly severe in a recent concept of an integral rocket–ramjet, where an initial solid propellant rocket is followed by a ramjet (or a ducted rocket) stage using large quantities of metallized particles burning with ambient air (Billig *et al.* 1980; Vanka *et al.* 1985). In both the above applications one encounters reacting solid particles. This paper deals with a direct numerical method to calculate the flow properties for a one-dimensional convergent–divergent nozzle having a reacting particle-laden gas as the flow medium. Such an approach enables one to easily compare results with the one-dimensional theory of pure gas flow. Although for a pure gas a one-dimensional approach forms part of any textbook on gas dynamics, evaluation of a two-phase flow theory for such a nozzle has developed very slowly, and to date the standard assumption is that the particles are non-reacting and that the particle drag and the heat transfer relations are the low Reynolds number (Stokes regime) expressions. Kliegel (1962) studied the case of constant particle velocity/gas velocity ratio (a similarity parameter), and various aspects of such flows were studied by Rudinger (1970) and Bose (1982). An interesting method by Hassan (1964) attempts to obtain a nozzle shape from a given distribution of the similarity parameter. However, such analyses invariably lead to impractical nozzle shapes. A direct numerical method for a one-dimensional two-phase flow was presented by Hultberg & Soo (1965), and was reported again by Soo (1967) for a very special nozzle. The method fails in the general case because of the difficulty in estimating the location of the point of singularity at the point of sonic crossing, which in a particle-laden gas flow is downstream of the nozzle throat, with any desired accuracy. Therefore it is conjectured that a time-dependent equation system, which is a hyperbolic-type equation system and is not dependent on whether the flow is subsonic, transonic or supersonic, is most suited for analysis of a two-phase system. In the present paper the governing equations, including the particle reaction terms, are nondimensionalized and more accurate particle drag and heat transfer laws are used, thus relaxing the low Reynolds number approximations used by other authors. Finally, a numerical solution for a fully conservative equation system is described and the numerical results presented. For this purpose an effort is made to balance various interaction terms in the mass, momentum and energy conservation equations for both gas and particles, and thus the method is slightly different from that used by Sharma & Crowe (1978).

2. ANALYSIS

The underlying assumptions of the present analysis are as follows:

1. There are no viscous or heat transfer effects for those associated with the drag and heat transfer between the gas and the particles.
2. The particles are spherical and uniform in size at a given location, with diameter d_s, mass M_s, temperature T_s and material density ρ_s'.
3. The particles and the gas flow can be considered as being one-dimensional—their respective property values at any cross-section represent the average value across the section.
4. The gas obeys the ideal gas law.
5. The gas specific heat at constant pressure c_{pG}, the gas Prandtl number Pr_G and the particle specific heat c_s are all constant.
6. In the case of reacting particles the particle diameter is reduced and the reduced particle mass content is converted to gas.

The basic unsteady equations for each of the species j (gas, particle) are:

continuity,

$$\rho_{jt} + \nabla \cdot (\rho_j \mathbf{V}_j) = \dot{m}_{Rj}; \tag{1}$$

i-momentum,

$$(\rho_j V_{ji})_t + \nabla \cdot (\rho_j V_{ji} \mathbf{V}_j) = -\nabla p_j + F_{ji}; \tag{2}$$

and

internal energy,

$$(\rho_j e_j^\circ)_t + \nabla \cdot (\rho_j \mathbf{V}_j e_j^\circ) = -\nabla \cdot (p_j \mathbf{V}_j) + \mathbf{V}_s \cdot \mathbf{F}_j + \dot{Q}_j + \dot{Q}_{Rj}. \tag{3}$$

In the above equations ρ_j is the density of the jth species (j = s,G for solid and gas, respectively), $\mathbf{V}_j$ is the velocity vector for the jth species, p_j is the partial pressure of the jth species and $\mathbf{F}_j$ is the volumetric force acting on the jth species. Now the relation between the specific internal total energy of the species, e_j°, and the specific total enthalpy of the species, h_j°, is

$$e_j^\circ = h_j^\circ - \frac{p_j}{\rho_j}$$

and the energy equation for the species in terms of the specific total enthalpy is thus,

$$(\rho_j h_j^\circ - p_j)_t + \nabla \cdot (\rho_j h_j^\circ \mathbf{V}_j) = \mathbf{V}_s \cdot \mathbf{F}_j + \dot{Q}_j + \dot{Q}_{Rj}. \tag{4}$$

In [4], $\dot{Q}_j$ and $\dot{Q}_{Rj}$ are the interphase energy transfer rate and chemical energy addition rate of the jth species.

Multiplying the momentum equation by the respective velocity component and adding, gives

$$\left(\frac{\rho_j V_j^2}{2}\right)_t + \nabla \cdot \left(\frac{\rho_j \mathbf{V}_j V_j^2}{2}\right) = -(\mathbf{V}_j \cdot \nabla p_j) + \mathbf{V}_j \cdot \mathbf{F}_j. \tag{5}$$

Subtracting [5] from [3] and [4] we get

$$(\rho_j e_j)_t + \nabla \cdot (\rho_j \mathbf{V}_j e_j) = -p_j \nabla \cdot \mathbf{V}_j + \dot{Q}_j + \dot{Q}_{Rj} + (\mathbf{V}_s - \mathbf{V}_j) \cdot \mathbf{F}_j \tag{6}$$

and

$$(\rho_j h_j - p_j)_t + \nabla \cdot (\rho_j \mathbf{V}_j h_j) - (\mathbf{V}_j \cdot \nabla p_j) = \dot{Q}_j + \dot{Q}_{Rj} + (\mathbf{V}_s - \mathbf{V}_j) \cdot \mathbf{F}_j. \tag{7}$$

It is obvious that for solid particles $p_s = 0$. Further, in [1]–[7] the variables $\dot{m}_{Rj}$, $\mathbf{F}_j$ and $\dot{Q}_j$ have opposite signs for the gas and the particles; this is due to the mass rate of production, the drag

on the particles due to the difference in velocities between the particles and the gas, and the heat exchange between the gas and the particles due to the difference in the temperature between the particles and the gas. Thus, $\dot{m}_{Rj} = \pm\dot{m}_R$, $\mathbf{F}_j = \pm\mathbf{F}$ and $\dot{Q}_j = \pm\dot{Q}$, where the upper sign is for the particles and the lower sign is for the gas. Thus, from [4] with no chemical reaction and for a steady state,

$$\nabla\cdot(\rho_G h_G^\circ \mathbf{V}_G) + \nabla\cdot(\rho_s e_s^\circ \mathbf{V}_s) = 0.$$

For the calculation of $\dot{Q}_{Rj}$ it is assumed that a large fraction of the thermal energy released due to chemical reaction goes to the gas and the rest to the particles. Thus, for the gas,

$$\dot{Q}_{Rg} = \beta m_R \Delta H$$

and for the particles,

$$\dot{Q}_{Rs} = (1-\beta)\dot{m}_R \Delta H,$$

where β is the fraction of the chemical energy released going to the gas and ΔH is the chemical energy released per unit mass of the particle.

If n_s is the number density of the particles, the mass rate of production of the particles, $\dot{m}_{Rs}$, is

$$\dot{m}_{Rs} = \pi d_s^2 n_s \rho_s' \dot{d}_s = 3\rho_s \frac{\dot{d}_s}{d_s} \qquad [8]$$

and $\dot{d}_s$ is the rate of reduction of the particle diameter, d_s, per unit time (a negative quantity). This model, therefore, assumes that the solid particles vanish due to chemical reaction and do not get converted into different particles, e.g. metal particles becoming metallic oxide particles. We now estimate the other interaction terms.

Estimation of the interaction terms

At low Reynolds numbers Re in the Stokes regime, the drag coefficient c_{D0} and the Nusselt number Nu_0 are given by the relations

$$c_{D0} = \frac{24}{\mathrm{Re}} \qquad \text{and} \qquad \mathrm{Nu}_0 = \frac{\alpha d_s}{k_G} = 2,$$

where $\mathrm{Re} = \rho_G d_s (V_G - V_s)/\mu_G$. Two ratios are defined to characterize the drag coefficient and the Nusselt number with respect to their values at low Reynolds numbers. Herein μ_G is the dynamic viscosity coefficient of the gas,

$$f_D = \frac{c_D}{c_{D0}} \qquad \text{and} \qquad f_N = \frac{\mathrm{Nu}}{\mathrm{Nu}_0}.$$

The drag and the heat transfer for a single particle are

$$D_1 = \frac{c_D \rho_G (V_G - V_s)^2 \pi d_s^2}{8}$$

and

$$Q_1 = \pi\alpha d_s (T_s - T_G) = \pi k_G \mathrm{Nu} d_s (T_G - T_s).$$

Noting that the mass of a single particle is $M_{s1} = \pi\rho_s' d_s^3/6$, then the force and the energy balances in the Stokes regime give

$$M_{s1}\frac{dV_s}{dt} = D_{10} = \frac{c_{D0}\pi d_s^2 \rho_G (V_G - V_s)^2}{8}$$

and

$$M_{s1} c_s \frac{dT_s}{dt} = \dot{Q}_{10} = \pi k_G \mathrm{Nu}_0 d_s (T_G - T_s).$$

This gives two expressions for the velocity and the temperature changes in the Stokes regime:

$$\frac{dV_s}{dt} = \frac{18\mu_G(V_G - V_s)}{(\rho_s' d_s^2)}$$

and

$$\frac{dT_s}{dt} = \frac{12k_G(T_G - T_s)}{(\rho_s' c_s d_s^2)}.$$

In the above, k_G is the heat conductivity coefficient of the gas and T_j is the temperature of the jth species.

Assuming a step change of the gas velocity and the gas temperature at time $t = 0$, two relaxation times can be defined, one for the gas velocity and one for the temperature. The velocity relaxation time for the Stokes regime is

$$\tau = \frac{\rho_s' d_s^2}{(18\mu_G)}. \qquad [9]$$

With n_s being the number density of the particles, the mass density of the particles is $\rho_s = n_s M_{s1}$ and the volumetric force $\mathbf{F}$ and the heat exchange term $\dot{Q}$ are

$$\mathbf{F} = -n_s D_1 = \frac{\rho_s(V_G - V_s)}{(\tau f_D)}$$

and

$$\dot{Q} = -n_s \dot{Q}_1 = \frac{(\frac{2}{3})\rho_s k_G(T_G - T_s)}{(\mu_G \tau f_N)}.$$

The f_D and f_N relations used in the present paper are the drag and Nusselt number correction, and are defined as follows:

$$\text{Re} < 1000: \; f_D = 1 + 0.15\,\text{Re}^{0.687} \text{ (Rowe 1961)}$$

$$\text{Re} > 1000: \; f_D = 0.01833\,\text{Re}$$

$$f_N = 1 + 0.2295\,\text{Re}^{0.55}\text{Pr}^{0.33}.$$

One-dimensional nozzle flow

From [1]–[7] the following vector equation can be written for a one-dimensional two-phase nozzle flow:

$$\mathbf{E}_t + \mathbf{G}_x = \mathbf{H}, \qquad [10]$$

where

$$\mathbf{E} = \begin{Bmatrix} \rho_G A \\ \rho_G u_G \\ \rho_G h_G^0 - p_G \\ \rho_s A \\ \rho_s u_s \\ \rho_s e_s^0 \end{Bmatrix}, \quad \mathbf{G} = \begin{Bmatrix} \rho_G u_G A \\ \rho_G u_G^2 + p_G \\ \rho_G u_G h_G^0 \\ \rho_s u_s A \\ \rho_s u_s^2 \\ \rho_s u_s e_s^0 \end{Bmatrix} \quad \text{and} \quad \mathbf{H} = \begin{Bmatrix} \dot{m}_R A \\ \mathbf{F} \\ u_s\mathbf{F} + \dot{Q} + \beta\dot{m}_R \Delta H \\ -\dot{m}_R A \\ -\mathbf{F} \\ -u_s\mathbf{F} - \dot{Q} + (1-\beta)\dot{m}_R \Delta H \end{Bmatrix},$$

where

$$h_G^\circ = c_{pG}T_G + \frac{u_G^2}{2},$$

$$e_s^\circ = c_s T_s + \frac{u_s^2}{2},$$

$$F = \frac{\rho_s(u_s - u_G)}{(\tau f_D)},$$

$$\dot{Q} = \frac{(\frac{2}{3})\rho_s k_G(T_G - T_s)}{(\mu_G \tau f_N)}$$

and A is the cross-sectional area.

The mass rate of production term can be estimated assuming that the solid particles burn fully and get converted into the gaseous form. Let d_s be the particle diameter at a particular location, which can be calculated from the nozzle inlet particle diameter d_{s0} and the elapsed time up to the location under consideration from the relation

$$d_s = d_{s0} - \int bp_G^n \, dt, \qquad [11]$$

where b and n are burning rate parameters, and $r = bp_G^n$ is the burning rate. Thus, the rate of change of the diameter of the particle is $\dot{d}_s = -bp_G^n$. If the number density of the particles n_s remains constant through the nozzle, then from [8] and [11] we get

$$\dot{m}_{Rs} = -\frac{3\rho_s bp_G^n}{d_{s0} - \int bp_G^n \, dt} = -\frac{3\rho_s bp_G^n}{d_{s0} - \int \left(\frac{bp_G^n}{u_s}\right) dx}. \qquad [12]$$

It is obvious from [12] that the denominator must remain positive, which places limits on the value of n, the length of the nozzle and the value of b.

Non-dimensionalizing the equation

Equations are non-dimensionalized with the help of the following non-dimensional variables:

$$x^* = \frac{x}{L}, \quad t^* = \frac{Ut}{L}, \quad u_s^* = \frac{u_s}{U}, \quad u_G^* = \frac{u_G}{U}, \quad \rho_G^* = \frac{\rho_G R_G T^\circ}{p^\circ}, \quad \rho_s^* = \frac{\rho_s R_G T^\circ}{p^\circ}, \quad p_G^* = \frac{p_G}{p^\circ},$$

$$T_G^* = \frac{T_G}{T^\circ}, \quad T_s = \frac{T_s}{T^\circ}, \quad h_G^{\circ *} = \frac{h_G^\circ}{(c_{pG}T^\circ)}, \quad e_s^{\circ *} = \frac{e_s^\circ}{(c_{pG}T^\circ)}, \quad A^* = \frac{A_t}{A}, \quad \mathrm{Pr}_G = \frac{\mu_G c_{pG}}{k_G},$$

$$\dot{m}_R = \frac{\dot{m}_R R_G T^\circ L}{(p^\circ U)}, \quad F^* = \frac{FL}{p^\circ}, \quad \dot{Q}^* = \frac{\dot{Q}L}{(p^\circ U)}, \quad c^* = \frac{c_s}{c_{pG}}, \quad \Delta H^* = \frac{\Delta H}{(c_{pG}T^\circ)}, \quad C_F = \frac{U\tau}{L},$$

$$K_1 = \frac{(\gamma - 1)}{(2\gamma)}, \quad K_2 = \frac{Ud_{s0}}{(Lr_0)} \quad \text{and} \quad U = \sqrt{2c_{pG}T^\circ}.$$

Thus, one gets

$$h_G^{\circ *} = T_G^* + u_G^{*2},$$

$$e_s^{\circ *} = c^* T_s^* + u_s^{*2},$$

$$F^* = \frac{\rho_s^*(u_G^* - u_s^*)}{(C_F f_D K_1)}$$

and

$$\dot{Q}^* = \frac{\rho_s^*(T_G^* - T_s^*)}{(3K_1 f_N \mathrm{Pr}_G C_F)};$$

and for chemical reaction,

$$\dot{m}_R^* = \frac{6p_G^*}{\left[K_2 - \int \left(\frac{p_G^{*n}}{u_s^*}\right) dx^*\right]}.$$

The non-dimensional form of [10] is now

$$E_t^* + G_t^* = H^*, \qquad [13]$$

where

$$\mathbf{E}^* = \begin{Bmatrix} \frac{\rho_G^*}{A^*} \\ \rho_G^* u_G^* \\ \rho_G^* h_G^{\circ *} - 2K_1 p_G^* \\ \frac{\rho_s^*}{A^*} \\ \rho_s^* u_s^* \\ \rho_s^* e_s^{\circ *} \end{Bmatrix}, \quad \mathbf{G}^* = \begin{Bmatrix} \frac{\rho_G^* u_G^*}{A^*} \\ \rho_G^* u_G^{*2} + K_1 p_G^* \\ \rho_G^* u_G^* h_G^{\circ *} \\ \frac{\rho_s^* u_s^*}{A^*} \\ \rho_s^* u_s^{*2} \\ \rho_s^* e_s^{\circ *} u_s^* \end{Bmatrix}$$

and

$$\mathbf{H}^* = \begin{Bmatrix} \frac{\dot{m}_R^*}{A^*} \\ K_1 F^* \\ 2K_1(u_s^* F^* + Q^*) + \beta \Delta H^* \dot{m}_R^* \\ \frac{-\dot{m}_R^*}{A^*} \\ -K_1 F^* \\ -2K_1(u_s^* F^* + Q^*) + (1-\beta)\Delta H^* \dot{m}_R^* \end{Bmatrix}.$$

Equation [13] is now a non-dimensional partial differential equation of hyperbolic type with respect to time, which has to be solved. In the above K_1 and K_2 are constants and β is the fraction of chemical energy going to the gaseous phase.

3. RESULTS AND DISCUSSION

Solution of [13] was obtained using the MacCormack (1969) explicit predictor–corrector scheme. Herein a fourth-order damping term with a damping coefficient of 0.1 was used to suppress non-linear instabilities. A standard three-point smearing technique using 95% weighting on the point under consideration and 2.5% on either side was used to smooth the flow variables. The integration time step was determined by the following expression:

$$\Delta t = \mathrm{CFL} \cdot \Delta x / |u + a|,$$

in which CFL is the Courant–Freidrich–Lewy number. With a reactive flow, it is necessary to use a smaller time-marching step. Typically, CFL was taken as 0.001.

The initial conditions for this problem were obtained using a one-dimensional isentropic flow analysis based on the average mixture properties. Subsequently, the individual phase arrays are obtained from the velocity lag K, and the mass fraction m^* assumed. Thus, the initial conditions bear the following relationship between the phases:

$$u_s^* = K \cdot u_G^*, \qquad m^* = \frac{(\rho_s^* \cdot u_s^*)}{(\rho_G^* \cdot u_G^*)} \qquad \text{and} \qquad T_s^* = 1 - L \cdot (1 - T_G^*),$$

where L is the temperature lag, and can be expressed as a function of K.

The exit boundary condition is based on a simple linear extrapolation of the conservation variables represented in vector **E*** of [13]. Since the exit flow was observed to be always supersonic, this treatment of the exit boundary was found to be satisfactory. The inlet boundary condition uses a much simpler method as compared to the characteristic formulation. The reservoir condition is associated with a large value of $A/A_{\text{throat}} = 10$. The stagnation pressure and the temperature are fixed at reservoir values but the velocity is allowed to develop as a part of the solution by backward linear extrapolation. Finally, the density is evaluated from the equation of state. This method was used by Anderson (1970) for time differencing quasi-one-dimensional equations.

The convergence criteria used here dictates that the relative error in the throat Mach number is $< 1 \times 10^{-4}$ and the relative error in the throat mass flow rate is $< 1 \times 10^{-5}$ in consecutive integrations. For this study, flow through a JPL axisymmetric nozzle with 45° entrance and 15° straight wall exit sections is considered. Details of this nozzle are shown in figure 1. The flow field is divided in 22 equally-spaced grid points and the converged solution requires approx. 400 integration steps for all the cases presented here.

Typical data used in this study are as follows: $T^\circ = 555.5\,\text{K}$, $p^\circ = 1.034 \times 10^6\,\text{Pa}$, $b = 4.5 \times 10^{-6}\,\text{m/(Pa)}^n$, $n = 0.5$ (burning rate is 4.5 mm/s at $1.034 \times 10^6\,\text{Pa}$ pressure), $\gamma = 1.4$, $c_p = 1070\,\text{J/kg K}$, $\text{Pr}_G = 0.74$, $\mu^\circ = 2.68 \times 10^{-5}\,\text{kg/m s}$ and $\Delta H = 2.7 \times 10^7\,\text{J/kg}$.

Figure 2 shows the computed Mach number variation and the pressure variation through the nozzle for a reactive flow with a solid particle of size of 20 μm. The sonic flow occurs downstream of the throat, which is located at the non-dimensional axial distance of 0.6. The Mach number and the pressure variation exhibit a similar trend for all the other cases investigated. Thus, for subsequent studies the Mach number at two locations, namely the throat and the exit, are used as parameters for comparison. This is adequate since the thrust developed depends essentially on the exit Mach number.

Figure 3 shows the throat Mach number as a function of the initial solid particle diameter d_{s0}. If the particles are nonreacting the throat Mach number is almost independent of the particle size for the size range considered. In the case of reactive particles: (a) the solid size changes through the pressure-dependent burning rate law; (b) the interphase momentum and heat transfer not only depend on the velocity difference between the two phases but also on the instantaneous particle size; (c) the solids gasify, adding to the mass of the gaseous phase; and (d) the combustion of solids adds heat to both the gaseous and solid phases in arbitrary proportions. As a consequence of the above, the reactive particles cause a greater throat Mach number variation as compared with the inert ones. This is especially true for smaller sized particles. This can partially be explained by the fact that the interphase transfer terms, as well as the source terms, are inversely proportional to the square of the size of the solid particles.

Figure 4 depicts the exit Mach number variation with respect to the solid size. Here the trend is similar to that seen in figure 3. In the case of reactive flow the exit Mach number is 1.917 for 10 μm size particles compared with 1.967 for 50 μm particles.

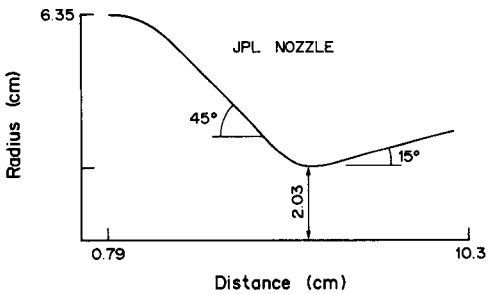

Figure 1. Shape of the JPL nozzle used for the calculation.

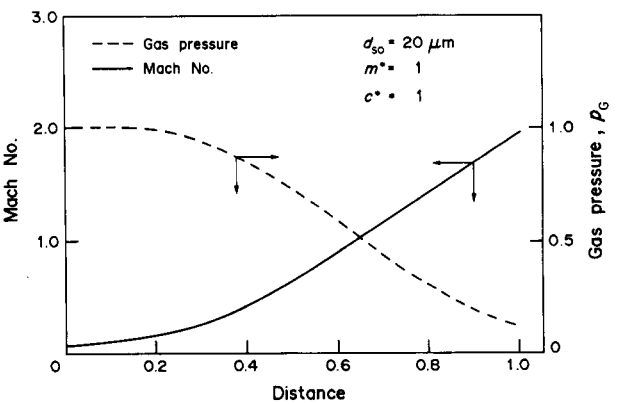

Figure 2. Mach number and pressure distribution in a nozzle.

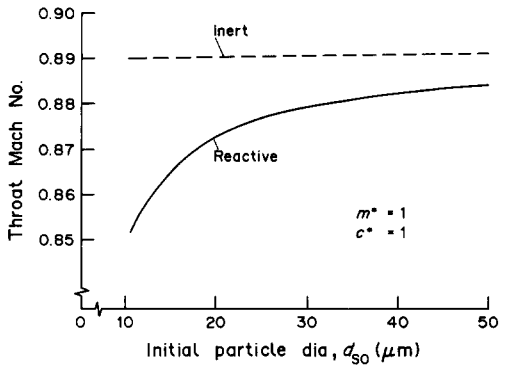

Figure 3. Throat Mach number vs initial solid diameter.

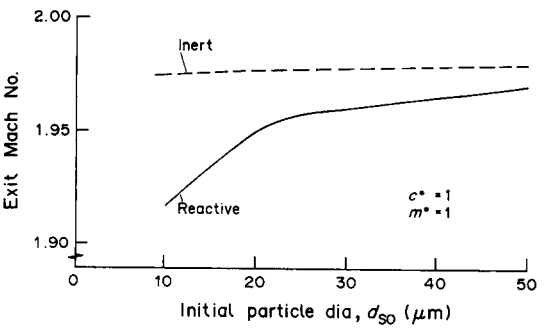

Figure 4. Exit Mach number vs initial solid diameter.

Figures 5 and 6 show the effect of the solid mass fraction m^* (defined as the ratio of the solid mass flux/gas mass flux at the inlet) on the Mach number. The mass fraction can also be defined in terms of the ratio of the solid mass/mixture mass (Chang 1980). Reduction in the mass fraction implies fewer solids and thus lower resistance on the gas flow. Thus, the throat and the exit Mach number are higher for lower mass fraction values. As shown in figure 5, the throat Mach number is considerably different for the inert and the reactive particles. However, as is evident from figure 6, there is very little difference between the two with regard to the exit Mach number, up to a mass fraction $m^* = 0.75$. The exit Mach number drops from a value of 2.3 at $m^* = 0.1$ to 2.0 at $m^* = 0.75$. Beyond this mass fraction, the difference is greater. In the case of the reactive particles, the exit Mach number reduces from 2.0 to 1.95 at $m^* = 0.1$.

Figures 7 and 8 show the variations of Mach numbers with respect to the ratio of solid/gas specific heat. Corresponding to the lower solid specific heat, the gas-phase Mach number is greater. Once again the throat Mach number shows greater variation between the reactive and the inert particles. When comparing the exit Mach number against the mass fraction variation, it is found that the exit Mach number is more sensitive to the specific heat ratio. For example, for $c^* = 1.5$, the exit Mach number remains supersonic, although it is reduced to 1.89.

4. CONCLUSIONS

Previous efforts reported in the literature have concentrated on the area of non-reacting solid–gas flow through nozzles. The present work investigated the effects of other important parameters, such as specific heat ratio and reacting particles, on one-dimensional two-phase flow through a nozzle.

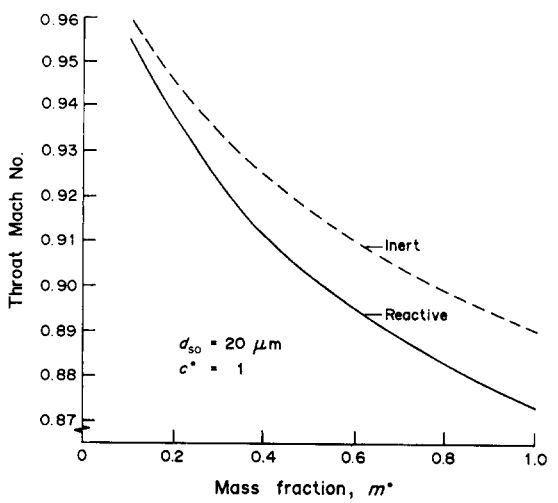

Figure 5. Throat Mach number vs mass fraction.

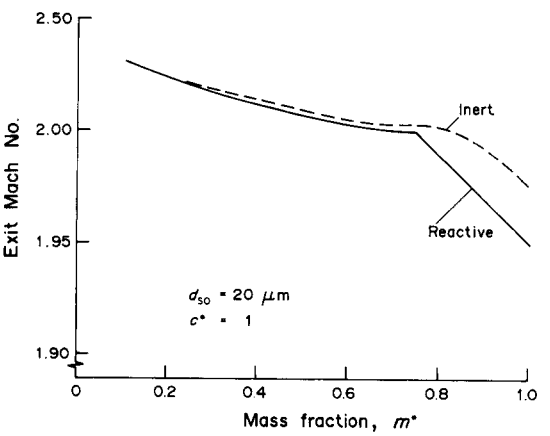

Figure 6. Exit Mach number vs mass fraction.

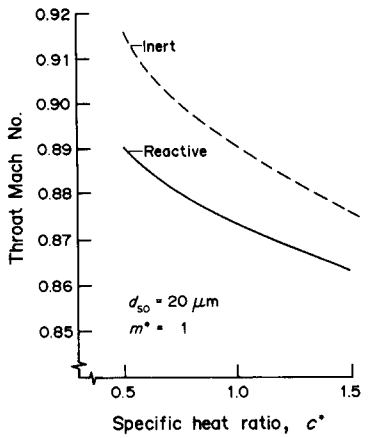

Figure 7. Throat Mach number vs non-dimensional specific heat ratio.

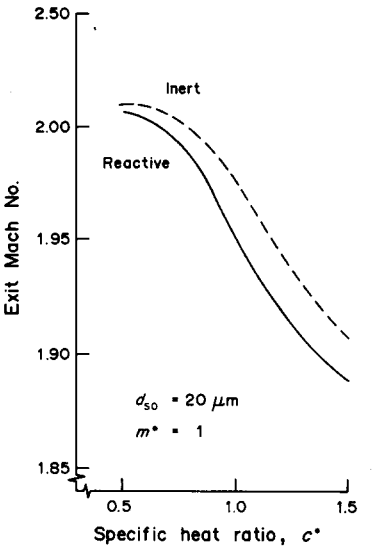

Figure 8. Exit Mach number vs non-dimensional specific heat ratio.

The following key conclusions have been reached from this study:

1. Smaller sized reacting solid particles slow down the gases considerably. As the initial particle diameter increases, the throat and the exit Mach number appear to be approaching a nearly constant value asymptotically.
2. As observed by other investigators, by suitably combining the solid loading with the solid size the exit Mach number can be suitably modified. This effect is enhanced in the case of reacting particles.
3. Variation of the specific heat of the particles has a marked effect on the exit Mach number.
4. Finally, the effect of the continued combustion of the solid particles throughout the nozzle results in a reduction of the gas velocity.

REFERENCES

ANDERSON, J. D. JR 1970 A time-dependent analysis for vibrational and chemical non-equilibrium nozzle flows. *AIAA Jl* **8,** 545–550.

BILLIG, F. S., WALTRUP, P. J. & STOCKBRIDGE, R. D. 1980 Integral rocket dual combustion ramjets: a new propulsion concept. *J. Spacecraft Rockets* **17,** 416–424.

BOSE, T. K. 1982 Thermodynamics of similar particle-laden gas flows in convergent–divergent nozzle. *J. Spacecraft Rockets* **19,** 376–378.

CHANG, I. S. 1980 One and two phase nozzle flows. *AIAA Jl* **18,** 1455–1461.

HASSAN, H. A. 1964 Exact solutions of gas–particle nozzle flows. *AIAA Jl* **2,** 395–396.

HESS, C. F. 1985 An instrument to measure the size and velocity of particles in a particle-laden flows. Report AIAA-85-1443.

HULTBERG, J. A. & SOO, S. L. 1965 Two-phase flow through a nozzle. *Astronautica Acta* **11,** 207–214.

KLIEGEL, J. R. 1962 Gas particles nozzle flows. In *Proceedings of the 9th International Symposium on Combustion*, pp. 811–826. Butterworths, London.

MACCORMACK, R. W. 1969 The effect of viscosity in hypervelocity cratering. Report AIAA-69-354.

ROWE, P. N. 1961 Drag forces in a hydraulic model of a fluidised model of a fluidised bed. Part II. *Trans. Instn chem. Engrs* **39,** 175–180.

RUDINGER, G. 1970 Gas–particle flow in convergent nozzles at high loading ratios. *AIAA Jl* **8,** 1288–1294.

SHARMA, M. P. & CROWE, C. T. 1978 A novel physico-computational model for quasi one-dimensional gas–particle flows. *ASME Jl Fluid Engng* **100,** 343–349.

Soo, S. L. 1967 *Fluiddynamics of Multiphase System.* Blaisdell, Waltham, Mass.

Vanka, S. P., Craig, R. R. & Stull, F. D. 1985 Mixing, chemical reaction and flow field development in ducted rockets. Report AIAA-85-1271.